Janus particles and interfacial activity

Miguel Angel Fernandez-Rodriguez[1,*], Miguel Angel Rodriguez-Valverde[2], Miguel Angel Cabrerizo-Vilchez[2], and Roque Hidalgo-Alvarez[2,†]

[1]*Laboratory for Interfaces, Soft Matter and Assembly, Department of Materials, ETH Zurich, Vladimir-Prelog-Weg 5, 8093 Zurich, Switzerland.*

[2]*Biocolloid and Fluid Physics Group, Applied Physics Department, Faculty of Sciences, University of Granada, 18071-E Granada, Spain.*

*e-mail: *ma.fernandez@mat.ethz.ch, †rhidalgo@ugr.es*

Janus particles are colloids with two different spatial domains. When these domains are synthesized with a contrast in wettability the particle show an enhanced interfacial activity in comparison with the corresponding homogeneous particles. There are different synthesis routes to fabricate such particles. One of the most common is to start with a homogeneous particle and functionalize just one hemisphere of the particle or form the particle directly with two compartments, the so called true Janus particles. Other particles which rely on the phase separation during synthesis are rather considered Janus-like particles. The Langmuir balance and the pendant drop tensiometry are useful to characterize the interfacial activity of the Janus and homogeneous particles at liquid interfaces.

Introduction

Pierre Gilles De Gennes was the first to coin the term Janus Particle (JP) to refer to anisotropic colloids with two spatial domains of different physicochemical properties (de Gennes, 1992). Depending on the differences between the spatial domains, the JPs can self-assemble or be responsive to external stimuli such as magnetic or electric fields, pH or temperature gradients (see Figure 1). In particular, if JPs are tailored with a contrast in wettability between both domains then the particles will present interfacial activity at fluid-fluid interfaces and they can be used, for instance, to stabilize Pickering emulsions.

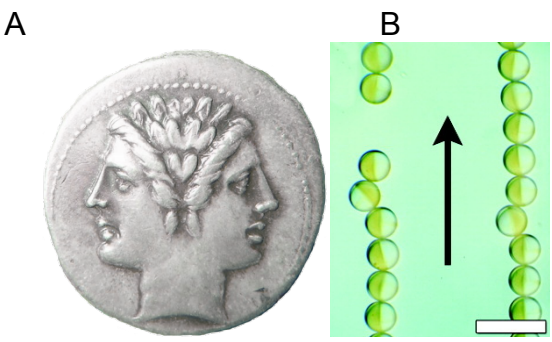

Figure 1. (A) Roman coin depicting the Janus god head. Public domain. (B) Hydrogel Janus particle with a superparamagnetic moiety self-assembled under a magnetic field in the arrow direction (100 μm scale bar). Adapted with permission from (Yuet et al., 2010). Copyright 2010 American Chemical Society.

This kind of interfacial-active JPs have been used as stabilizers of Pickering emulsions, to fabricate ultra-hydrophobic coatings, to emulsify and demulsify on demand with an external magnetic field if at least one spatial domain is loaded with magnetic iron oxide, as asymmetrical carriers for catalysis, for electronic paper, sensing and drug delivery.

When considering the advantages or disadvantages of JPs with interfacial activity, the first step is to compare them with the corresponding Homogeneous Particles (HPs). The HPs are entirely composed by one of the two components of the JP. For the following discussion it is useful to distinguish between surface activity and amphiphilicity. All particles are in principle surface active because when they are placed at the interface, the total area of the fluid-fluid interface is lower and this is energetically favorable. However, the particle will be more or less surface active depending on a great number of parameters such as its affinity towards both fluid phases, morphology, roughness, stiffness, etc (Perro et al., 2005 and Walther and Müller, 2008 and Jiang et al., 2010). On the other hand, only JPs with wettability contrast are amphiphiles since they present a dissymmetric surface with one moiety with more affinity towards one of the fluids and the other moiety towards the other fluid. In this case, the advantage is clear: 3-fold increase of the energy of adsorption of JPs compared to the corresponding HPs. This is a theoretical result that will be derived and described in the following section. Thus, the wettability anisotropy of JPs can stabilize Pickering emulsions for longer periods of time and under more stress (such as temperature changes or shear effects) rather than HPs. Amphiphilic JPs can further exhibit high interfacial activity regardless of the degree of amphiphilicity, due to the spatial separation of the different wettability regions (Binks, 2002), as can be seen experimentally in Figure 2.

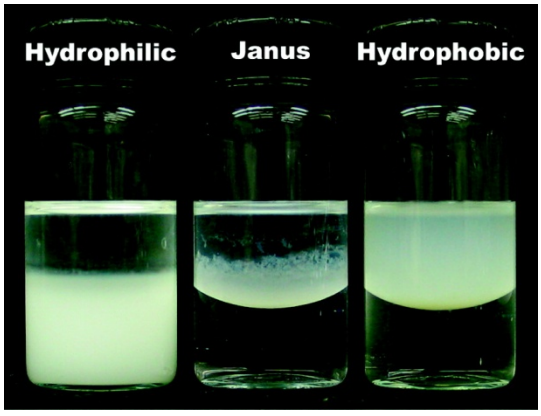

Figure 2. Plain, Janus, and fully modified silica particles with a silane dispersed in a mixture of water and toluene. The unmodified particles partitioned into the water phase (left panel), and the homogeneously hydrophobic particles partitioned into the toluene phase (right panel). Amphiphilic Janus particles quickly adsorbed at the water/toluene interface but they were not dispersed in either water or toluene phase (middle panel). Particle diameter is 500 nm. Reprinted with permission from (Jiang et al., 2008). Copyright 2008 American Chemical Society.

Synthesis of Janus particles with interfacial activity

There are multiple routes to synthesize JPs with interfacial activity. The traditional way is to immobilize particles forming monolayers on substrates, at fluid-fluid interface or in emulsion drops and then to functionalize the “facing” surface region. In the case of immobilizing the particles at

substrates, the typical routes are by spin-coating (i.e. spreading a drop containing the particles on a substrate to obtain a packed monolayer) or by Langmuir-Blodgett depositions from water/air or water/oil interfaces (i.e. spreading the particles at the interface, compressing them with the barriers to get a packed monolayer and next, dipping vertically a substrate across the interface). At liquid-air interfaces, the particles are spread in a Langmuir trough, compressed with a barrier up to form a packed monolayer and functionalized from the bulk phase as illustrated in Figure 3A. At water/oil interfaces the surface functionalization can be also performed from the oil phase. Finally, in the emulsion route, the drops are typically wax in water and once that the outer part of particles covering the colloidosome (see Figure 3B) is functionalized, the wax is melted releasing the JPs (Hong et al., 2006). It is interesting to point that in both routes involving spreading at the interface or emulsion drops, the HPs are surface active as discussed before but after the functionalization they become amphiphiles because of their dissymmetric surface.

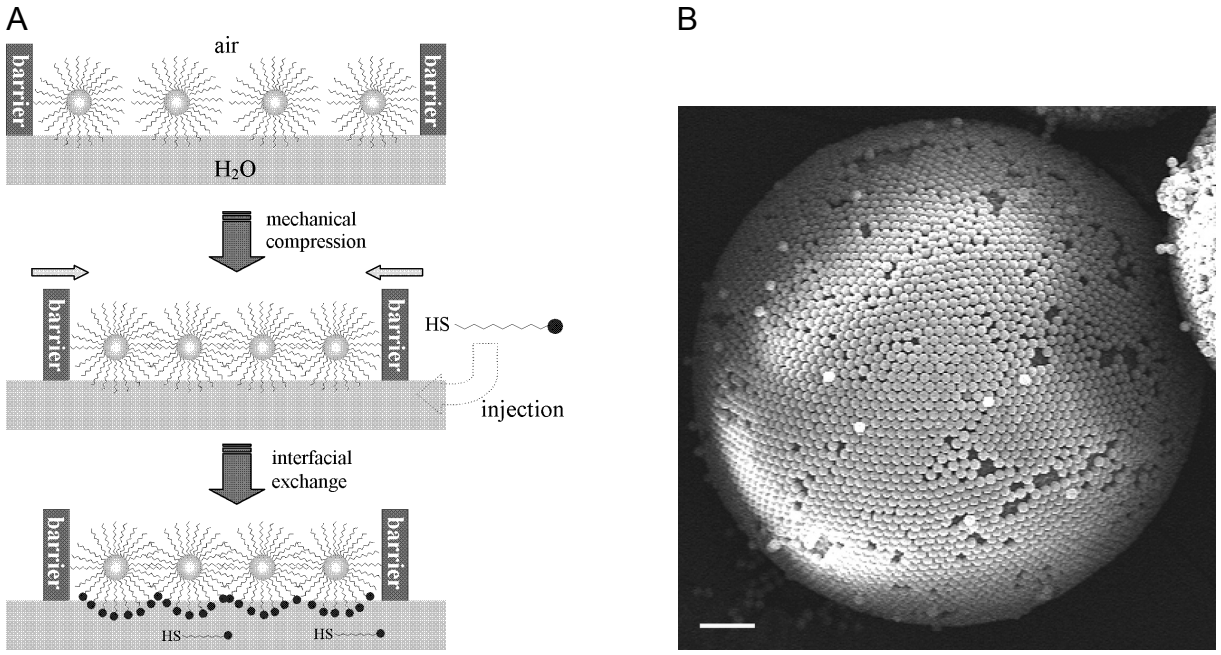

Figure 3. (A) Schematic of the preparation of Janus nanoparticles based on the Langmuir technique. Reprinted with permission from (Pradhan et al., 2007). Copyright 2007 WILEY-VCH. (B) SEM image of a silica particle-laden colloidosome before chemical modification. The wax used had a melting point of 53-57 °C. Particle diameter is 2 μm. Scale bar is 10 μm. Adapted with permission from (Jiang et al., 2008). Copyright 2008 American Chemical Society.

The aim of the synthesis recipes described above are inorganic particles, which are partially functionalized with a polymeric capping ligand or shell. Here, the Janus singularity is found onto the particle surface. Otherwise, there are routes to obtain JPs with two unlike volume halves. For example, partitioned organic JPs can be fabricated by converging two fine streams of different polymer solutions in a microfluidic channel and next, by UV-curing, the final spherical drops are solidified (see Figure 4A). However, only JPs in the range of microns are obtained with this method (Nie et al., 2006). To obtain smaller particles, electrohydrodynamic co-jetting can be used to accelerate nanoparticles of two segregated polymer solutions to a counter electrode by a voltage difference and the evaporation of the solvents produce a solid nanoparticle.

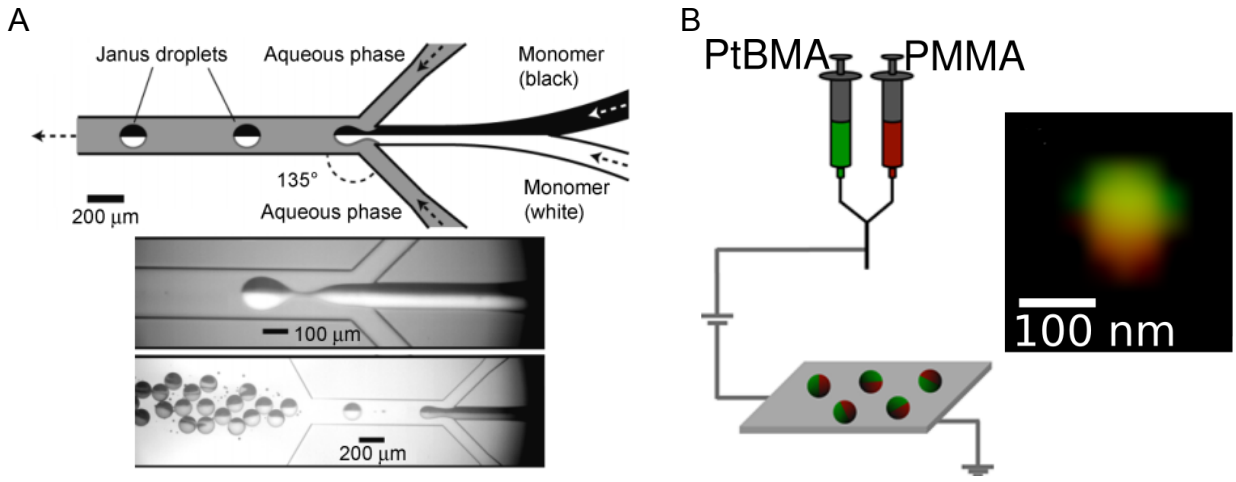

Figure 4. (A) Formation of bicolored Janus droplets in a planar microfluidic geometry. Layout of the channel and flow configuration (top) and experimental setup (bottom). Adapted with permission from (Nisisako et al., 2006). Copyright 2006 WILEY-VCH. (B) Schematic of Electrohydrodynamic co-jetting of Janus nanoparticles and super-resolution imaging of the Janus nanoparticles with Structured Illumination Microscopy. Reprinted from (Fernandez-Rodriguez et al., 2016), Copyright (2016), with permission from Elsevier.

The previously described JPs are usually referred as true Janus because the own synthesis validates the Janus nature. In contrast, other one-pot routes presume the spontaneous segregation of the capping ligands or of the two halves in bulk, accordingly. Due to this, some authors prefer to refer to them as Janus-like particles. Some one-pot synthesis routes can produce true JPs, usually with dumbbell morphology as seen in Figure 5. Controlling the polymerization of two different polymers, spherical or dumbbell JPs can be synthesized via the swelling of a cross-linked seed with a monomer which separates during polymerization. Even a simpler way is to take advantage of core-shell polymeric particles with a different cross-linker density in the core and the shell. Thus, a spatial separation occurs during cross-linking and it results in complex dumbbell morphologies. If one seeks to produce polymeric/inorganic particles with one-pot methods, both phases can be separated via ultrasonication, by electrostatic repulsion during polymerization or even the separation spontaneously occurs because of the growth of a crystal onto a core-shell microgel, which might lead to dumbbells of microgel-iron oxide crystal (see Figure 5).

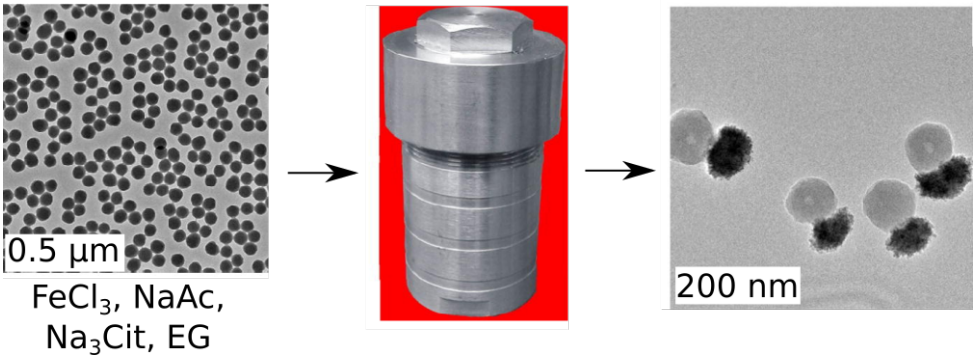

Figure 5. Hydrogel/Fe_3O_4 anisotropic Janus particles prepared through a one-pot process in the presence of the hydrogel microsphere as a template. Reprinted from (Liu et al., 2012), Copyright (2012), with permission from Elsevier.

Nevertheless, there is controversy about the Janus-like particles in the particular case of inorganic core covered with organic capping ligands. The spontaneous separation of the capping ligands at the

surface of the core predicted by some authors is supported and disproved in several works. For example, for silver cores functionalized with hydrophobic 1-undecanthiol and hydrophilic 11-mercaptoundecanoic acid, the capping ligands are spontaneously segregated in a Janus-like configuration, revealed with a significant macroscopic wettability contrast measured between both hemispheres of the particle deposited on a substrate (Sashuk et al., 2012). This is also supported with numerical simulations where randomly mixed thiolates segregate on gold nanoparticles up to a Janus configuration (Harkness et al., 2011). On the other hand, the opposite was found with neutron reflectivity (Reguera et al., 2015). In this study, a gold core functionalized with 1-octanethiol and 6-mercapto-1-hexanol at the water/air interface showed no rearrangement of the capping ligands. Thus, there was no Janus dissymmetry because the ligands were uniformly distributed on the gold surface (see Figure 6A). In a more recent work, gold nanoparticles with two randomly placed immiscible polymers as capping ligands, with different wettability, showed spontaneous segregation at the surface and a JP structure (Percebom et al., 2016). The spontaneously formed dissymmetry was verified with electron microscopy analysis in 2D and 3D as seen in Figure 6B.

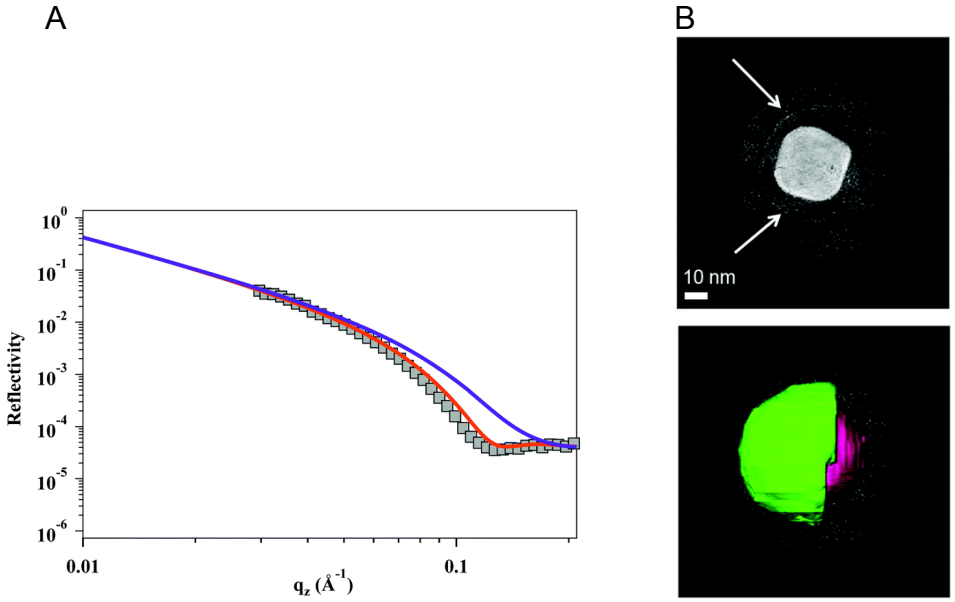

Figure 6. (A) Comparison of nuclear reflectivity profile of 1-octanethiol/6-mercapto-1-hexanol 1:1 coated gold nanoparticles at water/air interfaces (squares) with two models: assuming uniformly mixing in red and Janus dissymmetry in violet (Reguera et al., 2015) - Published by The Royal Society of Chemistry. (B) Bright field TEM tomography for nanoparticles coated by PEG 1 kDa + PNIPAM 1.2 kDa and stained with $CuSO_4$. Slices through the reconstruction show the shell around the particle (indicated by white arrows) dependent on the position of the slice. (Percebom et al., 2016) - Published by The Royal Society of Chemistry.

We demand techniques to discriminate if the new particle is true Janus or not. Different values of macroscopic wettability of two substrates covered, separately, with the particles with each half oriented up toward is an evidence of microscopic surface dissymmetry. Also NOESY-NMR (nuclear Overhauser effect spectroscopy used in nuclear magnetic resonance) is commonly used to show that there is no overlap of the patches of capping ligands at the particle surface, but this technique cannot resolve between a dissymmetric surface and a patched surface like a “football”. Besides, the study with neutron reflectivity explained above did not show a surface rearrangement, at least at water/air interface, of the capping ligands once the particles were placed at the interface. It becomes a non-

trivial task to characterize the Janus configuration as the particle size decreases. For large particles, it is possible to map their surface with super-resolution microscopy if both spatial domains are differently dyed (see Figure 4B). For particles up to 10 nm, we are able to map their surface composition by SEM or TEM (see Figure 6B) but for smaller particles it is necessary to use more advanced techniques as the mentioned NOESY-NMR, X-ray crystallography or ion mobility - mass spectrometry. Finally, if the JPs halves could not be distinguished by any technique, the Janus morphology should not be expected.

The synthesis routes described in this Section are widely used in literature. There is a vast amount of other developing techniques intended to synthesize JPs. For instance, when subjected to a flame inorganic particles of silica and iron oxide undergo a phase separation at high temperatures (Zhao and Gao, 2009). Exotic morphologies such as star-sphere anisotropic gold/iron oxide inorganic particles are also produced, which are used as probes for surface-enhanced Raman spectroscopy. This way they can improve the detection of the presence of molecules with very low concentrations (Reguera et al., 2016).

Theoretical aspects of Janus particles at fluid-fluid interfaces

The energy of desorption E_{des} of any particle at a fluid-fluid interface is given by the following equation:

$$E_{adsor} = \pi r^2 \gamma_{12}(1+\cos[(\theta_{12}))]^2 \quad E_{des} = \pi r^2 \gamma_{12} (1 \pm \cos\theta_{12})^2 \qquad (1)$$

where r is the particle radius, γ_{12} is the interfacial tension between both fluids and θ_{12} is the three-phase contact angle. The sign $\pm$ inside the bracket is negative for removal from the water (polar) phase, and positive for removal from the air or oil (non-polar) phase. Thus, the size appears to be very important and particles larger than a few nanometers can therefore be permanently attached to interfaces because of their greater energy of desorption. For example, a homogeneous particle of r = 10 nm adsorbed at the water/toluene interface (γ_{12} = 0.036 N/m) with θ_{12} = 90° has an energy of E_{des} = 2750 k_BT, thus it is irreversibly adsorbed.

Binks and Fletcher (2001) compared the energy of desorption of spheres of uniform wettability (HPs) and JPs adsorbed at an oil-water interface. The amphiphilicity of JPs can be tuned through the variation of both the angle α (which account for the relative areas of the polar and apolar domains, see Figure 7A) and the magnitude of the difference between the equilibrium contact angles, θ_A and θ_P, of the two domains of the particle adsorbed at the oil-water interface. The total surface free energy E of a JP at an oil-water interface as a function of the angle β (characterizing the immersion depth of the particle into the water phase, see Figure 7A) are given by:

For $\beta \leq \alpha$

$$E(\beta) = 2\pi r^2 \left[\gamma_{AO}(1+\cos\alpha) + \gamma_{PO}(cos\beta - cos\alpha) + \gamma_{PW}(1-cos\beta) - \frac{1}{2}\gamma_{OW}(\sin^2\beta) \right] \qquad (2)$$

and for $\beta \geq \alpha$

$$E(\beta)=2\pi r^2\left[\gamma_{AO}(1+\cos\beta)+\gamma_{AW}(cos\alpha-cos\beta)+\gamma_{PW}(1-cos\alpha)-\frac{1}{2}\gamma_{OW}(\sin^2\beta)\right] \qquad (3)$$

where r is the particle radius and γ_{AO}, γ_{PO}, γ_{AW}, γ_{PW} and γ_{OW} are the interfacial tensions of the apolar-oil, polar-oil, apolar-water, polar-water, and oil-water interfaces, respectively. Equations 2 and 3 assume a planar oil-water interface and a negligible line tension associated to the three-phase contact line around the particle. Moreover, Binks and Fletcher (2001) defined the $\theta_{average}$ as:

$$\theta_{average}=\frac{\theta_A(1+\cos\alpha)+\theta_P(1-\cos\alpha)}{2} \qquad (4)$$

As can be seen in Figure 7B, increasing the particle amphiphilicity through the $\Delta\theta=(\theta_P-\theta_A)/2$, the energy of desorption of the particles increases up to a maximum of 3-fold for $\Delta\theta=90^\circ$, corresponding to a JP. Moreover, the JPs maintain strong adsorption with $\theta_{average}$ around 0° or 180°, while the surface activity of the corresponding HPs is low.

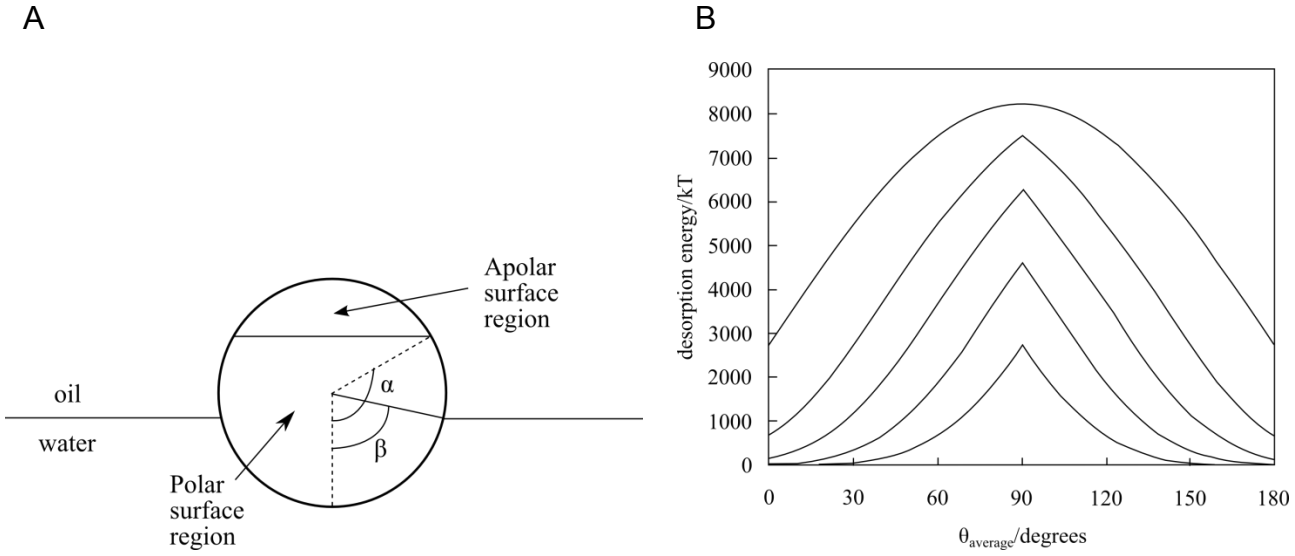

Figure 7. (A) Geometry of a Janus particle within an oil-water interface. The relative areas of the polar and apolar particle surface regions are parametrized by the angle α. The immersion depth of the particle through the oil-water interface is parametrized by the angle β. (B) Variation of particle desorption energy with area-weighted average contact angle for particles of radius 10 nm and α=90°. The oil-water tension was set to 36 mN m^{-1}. Increasing desorption energies correspond to $\Delta\theta$ varying from 0 (the homogeneous particle case), 20, 40, 60 to 90°. Both images reprinted with permission from (Binks and Fletcher, 2001). Copyright (2001) American Chemical Society.

Thanks to their large desorption energy, JPs can stabilize thermodynamically Pickering emulsions because the energetic balance can overcome the free energy increase for the formation of a bare oil-

water interface (Aveyard, 2012). This result takes into account lateral interactions between particles adsorbed at drop surfaces as electrical, hydration and van der Waals forces.

Regarding the shape of the JPs, Figure 8 shows results from simulations of the time evolution of interfacial tension of fluid-fluid interface by adsorbing Janus spheres, Janus rods and Janus discs at a fixed volume fraction. The interfacial tension showed a rapid decrease at early stages of adsorption for all JPs, but Janus spheres appear to be less efficient to decrease the interfacial tension and Janus disks the most efficient. Although there are experimental results pointing out to the same conclusions with JPs of similar geometries (Ruhland et al., 2013), the JPs were significantly different in size. It is recommended to conduct experimental studies with JPs with the same nominal size but different shape.

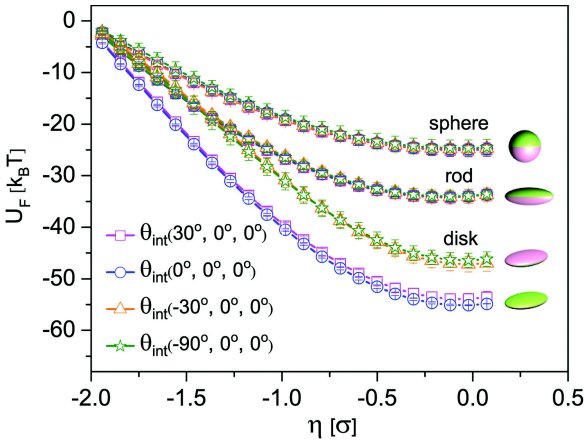

Figure 8. Time evolution of interfacial tension γ for JPs with different shapes. In these simulations, the aspect ratio of JPs is 1, 3.3, and 0.3 for Janus sphere, rod, and disk, respectively. Reprinted with permission from (Gao et al., 2014). Copyright [2014], AIP Publishing LLC.

Experimental results of Janus particles at fluid-fluid interfaces

To characterize the JPs at interfaces, it is essential that the JPs are in surfactant free conditions to characterize the interfacial activity without the interference of residual surfactants. There are two main measuring approaches: the microscopic one involving the direct measurement of the particle contact angle and the microstructure of the monolayers of JPs and the macroscopic one based on the interfacial tension measured with Langmuir balance or pendant drop tensiometry. The latter approach also enables to study macroscopic rheological properties of the monolayers subjected to different stresses.

Regarding the microscopic approach, there are different techniques as the Gel Trapping technique or the Freeze Fracture Shadow Casting cryo-SEM in which the particles are immobilized at the interface by a gel or by vitrification of the interface, respectively. Then, the contact angle of each particle is determined by SEM. For larger particles, de Gennes observed that JPs are attached at the interface with the plane separating both halves at the water/oil interface. For smaller particles this only happens in the case of large wettability contrasts (Synytska et al., 2014). For smaller wettability contrasts, the particles behave like HPs, with a contact angle coinciding with the contact angle of one of the parts of the surface. Thus, experimentally it is found that having two different functionalities on the particle surface do not necessarily lead to amphiphilic behaviour. Moreover, it is observed that JPs tend to assemble in fractal-like aggregates at oil/water interfaces due to attractive interactions.

Regardless of the macroscopic technique used, typically Langmuir balance or pendant drop tensiometry, the results of a vast variety of experimental studies validate the theoretical prediction: JPs present a higher interfacial activity (i.e. lower interfacial tension) compared to the corresponding HPs, as seen in Figure 9. Given the non-specialized character of this work, we point out the reader to the Further reading section for a more detailed discussion about experimental techniques and results.

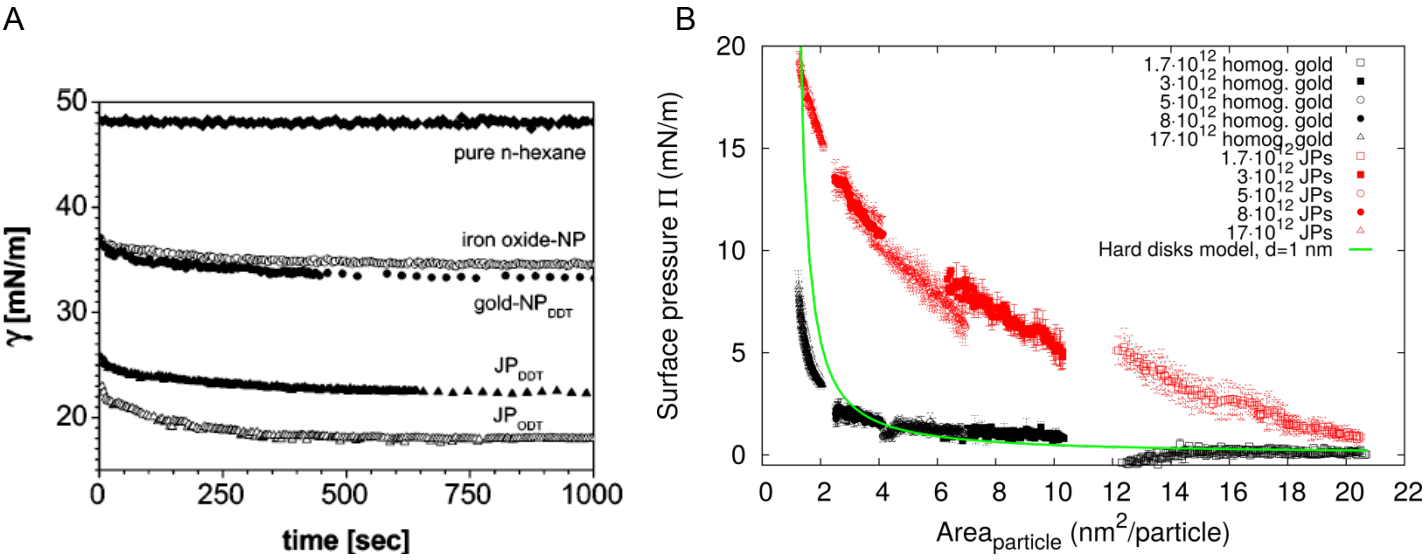

Figure 9. (A) Interfacial tension versus time. Nanoparticles adsorbing from the water bulk at the water/hexane pendant drop interface (NP: homogeneous nanoparticles; JP: Janus particles. The gold moieties were modified using dodecanethiol (DDT) or octadecanethiol (ODT)). Reprinted with permission from (Glaser et al., 2006). Copyright (2006) American Chemical Society. (B) Surface pressure against the area per particle for different number of gold JPs (red dots) functionalized by 2-(2-mercapto-ethoxy)ethanol and hexanethiol and HPs only functionalized with hexanethiol (black dots), deposited at the interface. Each black or red symbol corresponds to a single JP or HP deposition at the interface of the pendant drop. The solid line is the hard disks model for disks of 1nm diameter. Reprinted with permission from (Fernandez-Rodriguez et al., 2014). Copyright (2014) American Chemical Society.

Thanks to the Janus dissymmetry, self-propulsion of a gold/silica JP in bulk is achievable by self-thermophoresis. A laser beam focused to the JP creates a local temperature gradient at the gold-coated side of the particle which produces the motion by thermophoresis (Jiang et al., 2010). This self-propelling was recently observed with JPs half-coated with platinum (Wang et al., 2015) and it was predicted also by theoretical models of JPs trapped in a liquid-liquid interface (Malgaretti et al., 2016).

Finally, one can call into question if JPs are worth the effort despite of their complex synthesis processes. The response is that, mostly, JPs reveal enhanced interfacial activity at water/air and water/oil interfaces, compared to HPs.

Nomenclature

Symbols and Units

Da	Dalton, atomic mass unit.
T	Temperature
k_B	Boltzmann constant

	(=1.38064852×10^{-23} J K^{-1})
E_{des}	energy of desorption
r	particle radius
γ_{ij} γ_{12}	interfacial tension between *i*-phase and *j*-phase
θ_{12} θ_{12}	three-phase contact angle
α	angle that quantifies the relative particle areas of the polar and apolar domains.
β	angle that quantifies the immersion depth of the particle into the water (polar) phase
θ_A, θ_P	equilibrium contact angles of the polar and apolar domains of the particle adsorbed at the oil-water interface
E	total surface free energy
$\theta_{average}$	average contact angle
γ	interfacial tension

Abbreviations and Acronyms

JP	Janus Particle
HP	Homogeneous Particle
SEM	Scanning Electron Microscopy
UV	Ultraviolet
TEM	Transmission Electron Microscopy
PEG	PolyEthylene Glycol
PNIPAM	Poly(N-IsoPropylacrylAMide)
NOESY-NMR	Nuclear Overhauser Effect Spectroscopy-Nuclear Magnetic Resonance
cryo-SEM	Cryogenic Scanning Electron Microscopy

Keywords: **Janus particles** – **Anisotropic particles**: Synthesis of Janus particles: overview; **Surface and interfacial activity**: Surface activity and amphiphilicity, Particle-laden interfaces**; Fluid–fluid interfaces**: Energy adsorption, Langmuir balance, Pendant drop tensiometry

Acknowledgments

This work was supported by MINECO MAT 2016-78778-R, MAT2014-60615R, MAT 2013-44429-R and PCIN 2015-051 projects (MINECO and FEDER, Spain), by “Junta de Andalucía” and FEDER (projects P10-FQM-5977 and P12-FQM-1443). M. A. F. R. acknowledges financial support from the Swiss Government Excellence Postdoc Scholarship 2016.0246.

References

Aveyard, R. (2012). Can Janus particles give thermodynamically stable Pickering emulsions? Soft Matter 8:5233-5240.

Binks, B.P. (2002). Particles as surfactants-similarities and differences. Current Opinion in Colloid Interface Science 7:21-41.

Binks, B.P. and Fletcher, P.D.I. (2001). Particles adsorbed at the oil-water interface: a theoretical comparison between spheres of uniform wettability and Janus particles. Langmuir 17:4708-4710.

de Gennes, P.G. (1992). Soft matter. Science 256, 495-497.

Fernández-Rodríguez, M.A., Rahmani, S., Chris, K.J. et al. (2016). Synthesis and interfacial activity of PMMA/PtBMA Janus and homogeneous nanoparticles at water/oil interfaces. Colloids and

Surfaces A: Physicochemical and Engineering Aspects. In press, DOI: 10.1016/j.colsurfa.2016.09.043.

Fernandez-Rodriguez, M.A., Song, Y., Rodriguez-Valverde, M.A. et al. (2014). Comparison of the Interfacial Activity between Homogeneous and Janus Gold Nanoparticles by Pendant Drop Tensiometry. Langmuir 30:1799-1804.

Gao, H.M., Lu, Z.Y., Liu. H, et al. (2014). Orientation and surface activity of Janus particles at fluid-fluid interfaces. Journal of Chemical Physics 141(13):134907.

Garbin, V., Crocker, J.C. and Stebe, K.J. (2012). Particles at interfaces. Journal of Colloid and Interface Science 387:1-11.

Glaser, N., Adams, D.J., Böker, A. et al. (2006). Janus particles at liquid-liquid interfaces. Langmuir 22(12):5227-5229.

Harkness, K. M., Balinski, A., McLean, J. A. and Cliffel, D. E. (2011). Nanoscale phase segregation of mixed thiolates on gold nanoparticles. Angewandte Chemie International Edition 50: 10554-10559.

Hong, L., Jiang, S. and Granick, S. (2006). Simple method to produce Janus colloidal particles in large quantity. Langmuir 22: 9495-9499.

Jiang, H.R., Yoshinaga, N. and Sano, M. (2010). Active motion of a Janus particle by self-thermophoresis in a defocused laser beam. Physical Review Letters 105: 268302.

Jiang, S., Chen, Q., Tripathy, M. et al. (2010). Janus Particle Synthesis and Assembly. Advanced Materials 22: 1060-1071.

Jiang, S., Schultz, M.J., Chen, Q. et al. (2008). Solvent-free synthesis of Janus colloidal particles. Langmuir 24(18): 10073-10077.

Liu, B., Zhang, W., Zhang, D. et al. (2012). Facile method for large scale synthesis of magnetic inorganic–organic hybrid anisotropic Janus particles. Journal of Colloid and Interface Science 385(1): 34-40.

Malgaretti, P., Popescu, M.N. and Dietrich, S. (2016). Active colloids at fluid interfaces. Soft Matter 12: 4007-4023.

Nie, Z.H., Li, W., Seo, M. et al. (2006). Janus and ternary particles generated by microfluidic synthesis: Design, synthesis, and self-assembly. Journal of the American Chemical Society 128: 9408-9412.

Nisisako, T., Torii, T., Takahashi, T. et al. (2006). Synthesis of monodisperse bicolored Janus particles with electrical anisotropy using a microfluidic co-flow system. Advanced Materials 18:1152-1156.

Percebom, A.M., Giner-Casares, J.J., Claes, N. et al. (2016). Janus gold nanoparticles obtained via spontaneous binary polymer shell segregation. Chemical Communications 52: 4278-4281.

Perro, A., Reculusa, S., Ravaine, S., et al. (2005). Design and synthesis of Janus micro- and nanoparticles. Journal of Materials Chemistry 15: 3745-3760.

Pradhan, S., Xu., L. and Chen, S. (2007). Janus nanoparticles by interfacial engineering. Advanced Functional Materials 17:2385-2392.

Reguera, J., Jiménez de Aberasturi, D., Winckelmans, N., et al. (2016). Synthesis of Janus plasmonic-magnetic, star-sphere nanoparticles, and their application in SERS detection. Faraday Discussions, 191, 47-59.

Reguera, J., Ponomarev, E., Geue, T. et al. (2015). Contact angle and adsorption energies of nanoparticles at the air-liquid interface determined by neutron reflectivity and molecular dynamics. Nanoscale 7:5665-5673.

Ruhland, T.M., Grüschel, A.H., Ballard, N. et al. (2013). Influence of Janus Particle Shape on Their Interfacial Behavior at Liquid-Liquid Interfaces. Langmuir 29:1388-1394.

Sashuk, V., Hołyst, R., Wojciechowski, T. et al. (2012). Close-packed monolayers of charged Janus-type nanoparticles at the air-water interface. Journal of Colloid & Interface Science 375(1):180-186.

Synytska, A., Kirillova, A. and Isa, L. (2014). Synthesis and Contact Angle Measurements of Janus Particles. ChemPlusChem 79: 656-661.

Walther, A. and Muller, A.H.E. (2008). Janus particles. Soft Matter 4: 663-668

Yuet, K.P., Hwang, D.K., Haghgooie R. and Doyle, P.S. (2010). Multifunctional superparamagnetic Janus particles. Langmuir 26(6): 4281-4287.

Zhao, N. and Gao, M. (2009). Magnetic Janus particles prepared by a flame synthetic approach: synthesis, characterizations and properties. Advanced Materials 21: 184-187.

Further reading

Fernandez-Rodriguez, M.A., Rodriguez-Valverde, M.A., Cabrerizo-Vilchez, M.A. et al. (2016). Surface activity of Janus particles adsorbed at fluid-fluid interfaces: Theoretical and experimental aspects. Advances in Colloid and Interface Science 233:240-254.

Yoshida, M. and Lahann, J. (2008). Smart nanomaterials. ACS Nano 2(6), 1101-1107.

Reguera, J., Kim, H. and Stellacci F. (2013). Advances in Janus Nanoparticles. CHIMIA International Journal for Chemistry 67(11): 811-818.

Walther, A. and Müller, A.H.E. (2013). Janus particles: synthesis, self-assembly, physical properties, and applications. Chemical Reviews 113, 5194-5261.